PROCEEDINGS OF SCIENCE

https://ko.overleaf.com/project/64b58e80b2ffd323ab78232b

Correlation study using RHICf and STAR detectors to understand the finite transverse single spin asymmetry for very forward neutral pion production

Seunghwan Lee[a,b,*] **for the RHICf collaboration**

[a] *RIKEN*
2-1 Hirosawa, Wako, Saitama, Japan
[b] *Sejong University, Department of Physics,*
Seoul 05006, Republic of Korea

E-mail: zxzfdsa@gmail.com

Particles produced in the very forward region of hadronic collisions can contribute to the investigation of the origin of cosmic rays. In particular, Transverse Single-Spin Asymmetries (TSSA) provide insights for the particle production mechanism in terms of perturbative and non-perturbative strong interaction. The RHICf detector was added to the STAR detector system during the run in 2017 and collected data for polarized $p+p$ collisions at $\sqrt{s} = 510$ GeV. Previous studies with RHICf showed that asymmetries of the very forward π^0 meson, A_{N}, were observed to be non-zero for values in the range of $\eta > 6$, $p_{\mathrm{T}} < 1$ GeV/c. To further understand the origin of this result, we attempt to analyze the correlation between activities of very forward-rapidity and mid-rapidity regions, which are measured by RHICf and STAR detectors, respectively. In these proceedings, we will report the current status and future plan for this analysis.

38th International Cosmic Ray Conference (ICRC2023)
26 July - 3 August, 2023
Nagoya, Japan

*Speaker

PoS(ICRC2023)517

1. Introduction

The production process of particles with high transverse momentum at high energy polarized $p+p$ collision is related to the proton spin structure. Transverse Single-Spin Asymmetries (TSSA) can allow us to understand the production mechanism regarding perturbative and non-perturbative interaction. In theory, there are two theoretical frameworks, Transverse Momentum Distributions (TMD) and Twist-3 collinear factorization [1]. These two frameworks are based on QCD theory for The TSSA. The TMD framework requires the two scales known as transverse momentum p_T and large momentum transfer Q with $p_T << Q$ and the Twist-3 framework requires only the strong interaction scale, Λ_{QCD} with $p_T >> \Lambda_{QCD}$. Also, bath frameworks explain the same physics at $\Lambda_{QCD} << p_T << Q$ region [2]. The TSSA can be generated by spin-correlated TMD fragmentation at transverse q polarization in a transversely polarized proton [3]. For this reason, these frameworks can explain the large TSSA at high energy polarized $p+p$ collision [4]. TSSA (A_N) is quantified with a left-right cross-section asymmetry, $A_N = \frac{\sigma_L - \sigma_R}{\sigma_L + \sigma_R}$, where $\sigma_{L(R)}$ is the cross-section of a specific particle produced on the left (right) side relative to the beam polarization. This corresponds to the azimuthal asymmetry of particles produced in polarized $p + p$ collisions.

In 2017, the RHICf experiment collected data in $p + p$ collisions at $\sqrt{s}$ = 510 GeV with the STAR experiment at the Relativistic Heavy Ion Collider (RHIC) [5]. The previous RHICf results observe a non-zero A_N measured with very forward π^0 within p_T < 1 GeV/c, pseudo-rapidity (η) > 6, which indicates that the diffractive processes may be involved [6]. Furthermore, this result raised an interesting question; despite the expectation that the measured TSSAs are from regions where different processes are expected to dominate, the tendency for them to increase along the longitudinal momentum fraction scale (x_F) is similar for most of the measurements within error. TSSA of the π^0 result had measured by STAR experiment using the STAR Forward Meson Spectrometer (FMS) within 2.6 < $|\eta|$ < 4.2, p_T range is 3 GeV/c to 7 GeV/c [7], and the other TSSA is in 0.07 < p_T < 0.69 for the RHICf's π^0. Another comparison result shows this trend more clearly [8]. Our aim is to answer the question of why these two TSSAs of the result are the same. To understand the origin of these phenomena, We will study the correlations for processes.

2. RHICf experiment

The RHICf experiment was designed to study cosmic-ray and spin physics by measuring particles in the very forward region with the RHICf detector [9]. The RHICf detector was initially based on an electromagnetic calorimeter developed from the Arm1 calorimeter for the LHCf experiment. In the year of 2017, the RHICf detector was installed 18 m away from the interaction point and in front of the ZDC [10] in the STAR detector system.

The RHICf detector consists of two position-sensitive calorimeters, namely TL (large tower, 40 mm in size) and TS (small tower, 20 mm in size). Each tower is composed of 4 layers of X-Y pairs of layers with multi-anode photomultiplier tube (PMT) readout for position measurement, 16 layers of 1 mm-thick GSO scintillators for energy measurement, and 17 layers of tungsten absorbers with a total of 44 radiation length.

The RHICf detector has an energy resolution of 2−3% and a position resolution of 100−150μm for 100–250 GeV photons. Two photons from π^0 decays can be detected in two different towers

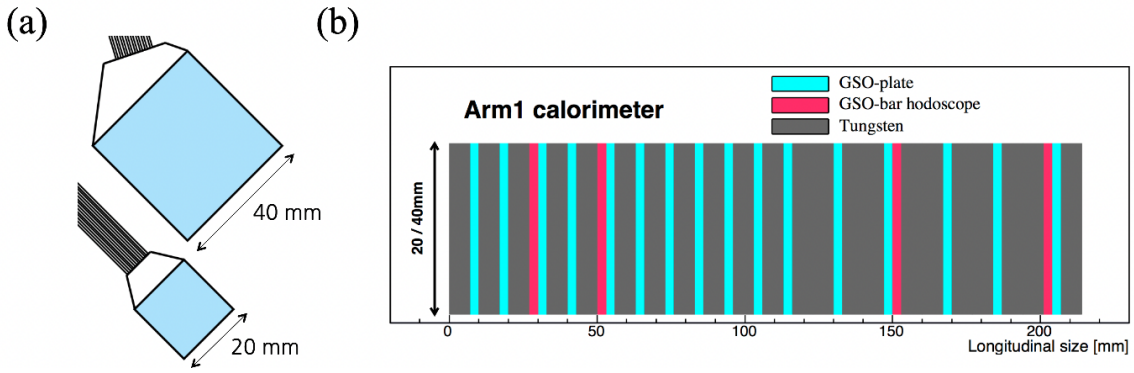

Figure 1: Schematic drawing of the (a) front view and the (b) longitudinal structure of the RHICf detector.

(type 1) or within one tower (type 2) [11]. For π^0, the energy resolution at energies of 100 – 250 GeV is 2.5 – 3.5% and the p_T resolution in the range of $0.0 < p_T < 0.8$ GeV/c is 3.0 – 4.5% for both types.

For the purpose of measuring a wide pT range, the detector operated with three different configurations; the beam entered 1) the center of TL, 2) the center of TS, and 3) 24 mm below the TS. The luminosity during RHICf operation was $\sim$ 1031 cm^2 s^{-1}, lower than that during typical RHIC operation with a small β^*.

Events used for the RHICf analysis are triggered by three separate trigger conditions; 1) when an electromagnetic (EM) shower occurs in only one RHICf tower, 2) when an EM shower occurs in two RHICf towers, 3) when there is a high EM hit. These trigger conditions are designed to measure decayed two photons from neutral pion and hadron. In addition, events triggered by STAR's general minimum-bias trigger conditions are used for reference.

3. Analysis status

To confirm the assertion that the origin of the very forward pi0's AN arises from a diffractive process rather than non-diffractive processes, the same measurement is replicated but more differentially. This is carried out in conjunction with data from other STAR sub-detectors.

The STAR experiment [12] includes several detectors, Time Projection Chamber (TPC), Barrel and End-cap EM Calorimeter (B-EEMC), Forward Mason Spectrometer (FMS), Beam Beam Counter (BBC), Vertex Position Detector (VPD), Event Plane Detector (EPD), Zero-Degree Calorimeter (ZDC), and Roman-Pots detector (RPS). Figure 2 shows the schematic of the STAR detectors with RHICf detector.

BBC, VPD, and ZDC cover η ranges, $2.2 < |\eta_{\mathrm{BBC}}| < 5.0$, $2.2 < |\eta_{\mathrm{VPD}}| < 5.0$, and $2.2 < |\eta_{\mathrm{ZDC}}| < 5.0$, respectively. These detectors are designed to be trigger detectors and also can be used in conjunction with TPC tracks to find the collision vertex. TPC and BEMC exist in $|\eta| < 1$ regions, and also EEMC is in $1 < |\eta| < 2$, these detectors are used to find the trajectory of charged particles and their energy. FMS that occupy $2.5 < |\eta| < 4.0$ can be analyzed for forward particle asymmetry and RPS ($7 < |\eta_{\mathrm{RPS}}| < 9$) was designed to analyze proton-proton elastic scattering. Also, the RHICf detector covered the range $|\eta| > 6$. The pseudo-rapidity gap between these detectors allows us to determine the process from which the asymmetry of π^0 originates.

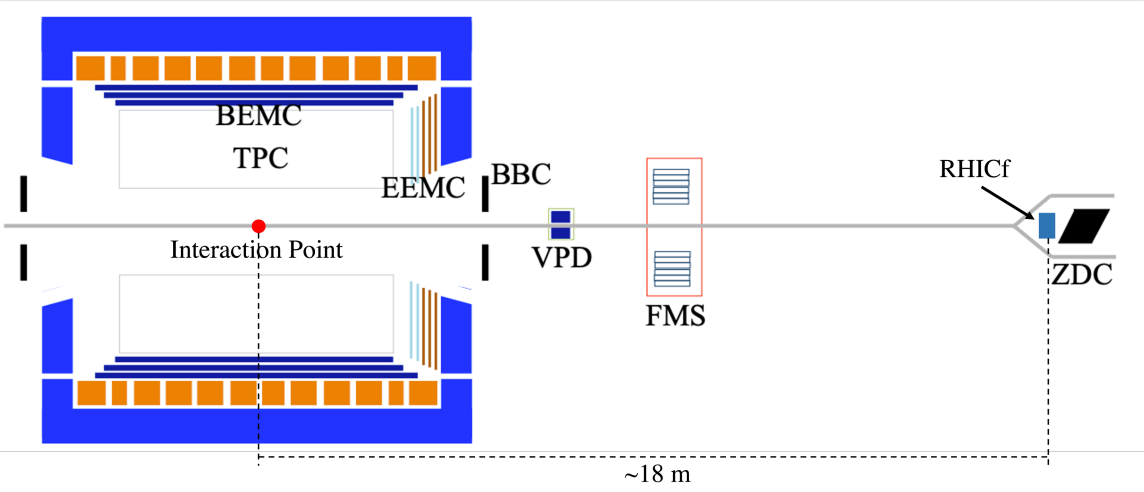

Figure 2: Schematic STAR sub-detectors and RHICf detector.

Currently, we have built the RHICf detector information and its reconstruction tool inside the STAR software library. Figure 3 shows the number of events triggered by RHICf triggers (left) and other STAR triggers (right) as a function of run period.

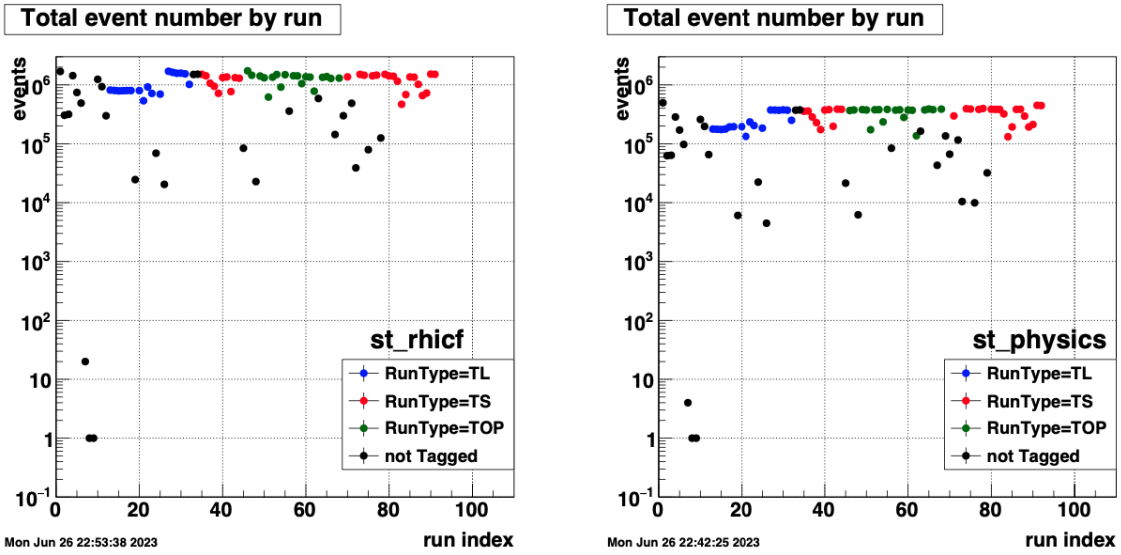

Figure 3: Total number of events, triggered by RHICf (left) and STAR triggers (right)

Each colored point represents RHICf run types, and the black points are not tagged as RHICf run types due to the poor beam condition, RHICf detector errors during the operation. These runs were not used in the previous RHICf results and will also be excluded from this study.

We also checked the kinematics of the reconstructed π^0 to see the performance of the RHICf reconstruction tool in the STAR library using tagged TS runs. Figure 4 shows p_T and x_F regions for type-1 and type-2 π^0. These π^0 are selected by the invariant mass and E_{π^0} energy ranges of 114 MeV/c^2 < $M_{\gamma\gamma}$ < 154 MeV/c^2, E_{π^0} > 50 GeV. it also indicates that most of π^0 measured within

p_T < 1 GeV/c and shows that p_T and x_F of π^0 are different depending on π^0 types due to definition of the π^0 types. We are currently reproducing the previous A_N results within the STAR software framework for validation.

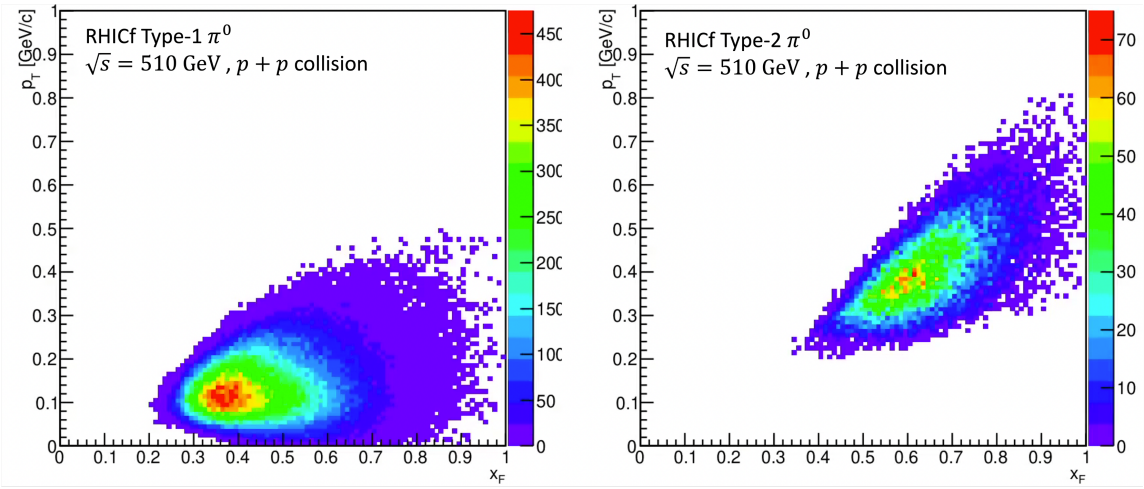

Figure 4: p_T and x_F dependence of type-1 (left) and type-2 (right) π^0

References

[1] J. Qiu, G. Sterman, *Phys. Rev. D* **59**, 014004 (1998).

[2] X. Ji, J.-W. Qiu, W. Vogelsang, and F. Yuan, *Phys. Rev. Lett.* **97**, 082002 (2006).

[3] J. Collins, *Nucl. Phys. B* **396**, 161 (1993).

[4] U. D'Alesio, F. Murgia, *Phys. Rev. D* **70**, 074009 (2004).

[5] RHICf Collaboration: LOI, arXiv: 1409. 4860v1.

[6] Minho Kim *et al.* (RHICf Collaboration), *Phys. Rev. Lett.* **124**, 252501 (2020).

[7] M. M. Mondal *et al.* (STAR Collaboration), *Proc. Sci.*, **DIS2014**, 216 (2014).

[8] J. Adam *et al.* (STAR Collaboration), *Phys. Rev. D* **103**, 092009 (2021).

[9] RHICf Collaboration, *JINST* **16** P10027 (2021).

[10] C. Adler *et al.*, *Nucl. Instrum. Meth. A* **470**, 488 (2001).

[11] O. Adriani *et al.* (LHCf Collaboration), *Phys. Rev. D* **94**, 032007 (2016).

[12] K. H. Ackermann *et al.* (STAR Collaboration), *Nucl. Instrum. Meth. A* **499**, 624 (2003).